

# Metallic Coatings for Enhancement of Thermal Contact Conductance

M. A. Lambert\* and L. S. Fletcher†  
Texas A&M University, College Station, Texas 77843

The reliability of standard electronic modules may be improved by decreasing overall module temperature. This may be accomplished by enhancing the thermal contact conductance at the interface between the module frame guide rib and the card rail to which the module is clamped. Some metallic coatings, when applied to the card rail, would deform under load, increasing the contact area and associated conductance. This investigation evaluates the enhancements in thermal conductance afforded by vapor deposited silver and gold coatings. Experimental thermal conductance measurements were made for anodized aluminum 6101-T6 and electroless nickel-plated copper C11000-H03 card materials to the aluminum A356-T61 rail material. Conductance values for the electroless nickel-plated copper junction ranged from 600 to 2800 W/m<sup>2</sup>K (105.7–493.1 Btu/h ft<sup>2</sup>°F), and those for the anodized aluminum junction ranged from 25 to 91 W/m<sup>2</sup>K (4.4–16 Btu/h ft<sup>2</sup>°F) for contact pressures of 0.172–0.862 MPa (25–125 psi) and mean junction temperatures of 20–100°C (68–212°F). Experimental thermal conductance values of vapor deposited silver- and gold-coated aluminum A356-T61 rail surfaces indicate thermal enhancements of 1.25–2.19 for the electroless nickel-plated copper junctions and 1.79–3.41 for the anodized aluminum junctions. The silver and gold coatings provide significant thermal enhancement; however, these coating-substrate combinations are susceptible to galvanic corrosion under some conditions.

## Nomenclature

$F$  = flatness  
 $H$  = hardness  
 $h$  = thermal conductance  
 $k$  = thermal conductivity  
 $R$  = roughness  
 $S$  = asperity slope  
 $t$  = coating thickness  
 $W$  = waviness

### Subscripts

$a$  = centerline average (CLA)  
 $c$  = coated, coating  
 $q$  = root mean square (rms)  
 $s$  = substrate  
 $u$  = uncoated

## Introduction

THE increasing demand for reliable electronic devices and systems for use over a broad range of environmental conditions requires the development of electronic systems which will meet higher performance standards. The heat generation within these devices is one of the primary factors which limit the ultimate thermal performance of individual components.<sup>1</sup> High junction temperatures and the associated thermal environment lead to overheating, reducing component performance, and increasing the possibility of thermally induced failure. In many instances, these failures may be related to the thermal resistance between the subcomponents or components within the system, such as the thermal resistance between standard electronic module (SEM) guide ribs and

card rails. As a consequence, there is an increasing interest in enhancing the heat transfer at interfaces within electronic systems.

One approach is to decrease the module overall operating temperature by reducing the thermal resistance between the module guide rib and card rail chassis (Fig. 1). This may be accomplished by increasing the apparent contact pressure, increasing the area of contact between the guide rib and card rail through system redesign, or through some form of surface treatment which deforms to increase the area of contact. A reduction in the thermal contact resistance will improve the heat transfer at the guide rib/card rail interface and decrease the guide rib temperature and the overall module temperature.

System redesign to augment the apparent contact area may not be practical, as this might incur significant expense in retrofitting systems already in service in order to accommodate new components. An increase in apparent contact pressure may not be feasible, since increased loads may damage or distort components. Specification of smoother, flatter surfaces may not be technically or economically possible due to

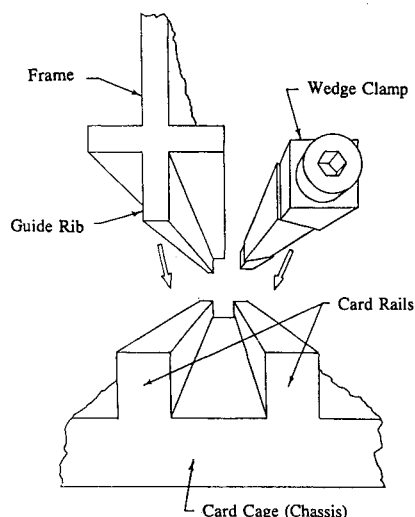


Fig. 1 Schematic of a typical guide rib/card rail interface.

Received June 11, 1992; presented as Paper 92-2849 at the AIAA 27th Thermophysics Conference, Nashville, TN, July 6–8, 1992; revision received May 18, 1993; accepted for publication May 24, 1993. Copyright © 1993 by the American Institute of Aeronautics and Astronautics, Inc. All rights reserved.

\*Graduate Research Assistant, Conduction Heat Transfer Laboratory, Department of Mechanical Engineering. Student Member AIAA.

†Thomas A. Dietz Professor, Conduction Heat Transfer Laboratory, Department of Mechanical Engineering. Fellow AIAA.

the limitations of extrusion and machining operations and the expense of grinding or lapping components to a fine finish. Foil inserts are difficult to handle, and may wrinkle during insertion, thereby possibly increasing the contact resistance. Consequently, one of the most effective techniques for enhancing heat transfer at an interface involves the treatment of the contacting surfaces. These treatments include surface preparation as well as the addition of chemically deposited or vapor deposited materials on the surfaces. For thermal enhancement, metallic coatings are generally the most successful surface treatment.

Although the physical phenomena involved in the use of thin metallic coatings to enhance the thermal contact conductance are not well understood, metallic coatings have several desirable characteristics. First, they are relatively easy to handle once applied and will not wrinkle or fold; second, under normal operating conditions they are stable in a vacuum environment; and third, the vapor deposition, sputtering, and/or electroplating processes used to apply these coatings are well understood and allow thin layers of almost any material or combination of materials to be deposited in the desired thickness. When soft metals are deposited on a surface, the metal coating will deform when placed in contact with a harder surface, thereby increasing the contact area.

There have been a number of investigations dealing with the thermal contact conductance of metals with metallic coatings.<sup>2-12</sup> O'Callaghan et al.<sup>6</sup> and Antonetti and Yovanovich<sup>8</sup> provide analytical correlations for estimating the contact conductance of nominally flat, rough surfaces. However, as previously described,<sup>13</sup> these correlations are not generally applicable to data in the remainder of these investigations. In addition, these correlations utilize surface asperity slope as a parameter. This surface characteristic is more difficult to specify in drawings and measure in a manufacturing environment than roughness or flatness. Consequently, it is still necessary to experimentally determine the contact conductance of the particular junction being evaluated.

Because the purpose of this investigation is to identify and evaluate conductance enhancing metallic coatings for electronics subjected to severe environments, attention is given to those metallic coatings that would not only increase conductance, but also resist wear in sliding contacts and galvanic corrosion. Gold and silver were selected as the most suitable metallic coating materials by reason of their low hardness, high thermal conductivity, and excellent corrosion resistance.<sup>13</sup>

Several investigations<sup>6,8,10,11</sup> suggest that an optimal coating thickness exists which is typically on the order of the root mean square average of the roughness of the two surfaces in contact. Contact conductance increases with coating thickness up to this optimal value because of the increased plastic deformation of the coating resulting from the reduced effective microhardness of the coating/substrate combination. For coating thickness greater than this optimal value, the interfacial resistance increases due to the increased bulk resistance of the coating. The optimal coating thicknesses for silver and gold were determined as part of this investigation.

It is typically more advantageous to coat the smoother of the two contacting surfaces, since coating of the rougher surface would result in a large amount of material being deposited between the peaks of the microscopic asperities (surface irregularities) where it will not contact the smoother surface. However, in this investigation the card rail material was coated with gold and silver without regard as to whether the card rail specimens were smoother than the guide rib specimens.

The present experimental investigation is directed toward measurement of the thermal contact conductance for junctions of anodized aluminum 6101-T6 and electroless nickel-plated copper C11000-H03 to aluminum A356-T61, and then toward determination of the conductance values for several thicknesses of vapor deposited gold and silver coatings on aluminum A356-T61 surfaces. This permitted determination

of the level of conductance enhancement provided by the coatings as well as the optimal coating thicknesses. A more detailed account of this experimental program was reported by Lambert and Fletcher.<sup>14</sup>

### Experimental Program

An experimental investigation was conducted to determine the thermal conductivity of the three base materials used in SEM cards and guide rails, and the thermal contact conductance of the junctions between these materials with the specified coatings. The experimental test facility, materials and coating preparation, mechanical and thermal property measurements, test procedure, and measurement uncertainty are all discussed.

### Experimental Facility

The experimental apparatus consists of a frame for supporting a column of 2.54-cm- (1-in.-) diam cylindrical specimens contacting at their ends, as shown in Fig. 2. The fixtures which hold the specimens are each equipped with a cluster of three 200-W Watlow cartridge heaters and a cooling coil through which refrigerated ethylene glycol from a constant temperature bath may be circulated. Consequently, the heat flux may pass either direction through the column, depending upon which cluster of heaters and cooling coil are activated. The apparent interfacial pressure is controlled by pressurizing a gas bellows attached to the upper movable plate of the frame. Load is transmitted to the specimen holding fixtures through large ball bearings. This ensures uniform loading of the test interfaces. The cooling coils are supplied by flexible hoses so as to eliminate any significant lateral thrust on the test column which would create a bending moment and result in uneven interfacial loading. The load is measured by a 2200-N (500-lb) capacity Eaton load cell which has been dead weight calibrated over the load range of interest, 0–445 N (0–100 lb). This load range provides an apparent contact pressure range of 0–862 kPa (0–125 psi) for axial contact of 2.54-cm- (1.0-in.-) diam cylindrical specimens.

The entire facility is enclosed in a vacuum chamber which is held at less than  $10^{-5}$  Torr to minimize convective heat

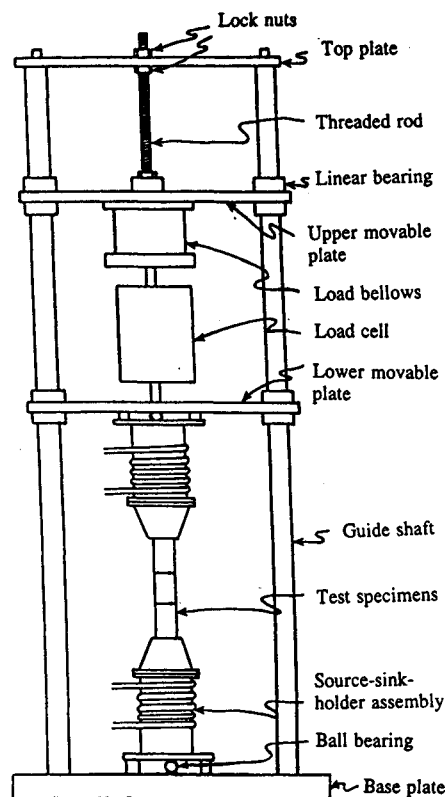


Fig. 2 Experimental test facility.

losses. The vacuum is maintained by an Alcatel 2300 roughing pump in series with a Varian VHS-6 oil diffusion pump. The vacuum level is measured with a Monitorr 2000 ion gauge controller. The test samples are surrounded by a cylindrical passive radiation shield. The shield is made of highly reflective aluminum foil. It contains ring-shaped inserts located adjacent to the specimen interfaces to reduce radiation exchange between specimens.

#### Materials

The base materials and surface finishes specified for this research investigation are as follows:

1) Aluminum frame: Aluminum alloy 6101-T6, extrusion base material; the surface finish is a hard black anodic coating with a surface roughness of  $0.6 \mu\text{m}$  ( $24 \mu\text{in.}$ ) and a surface flatness of  $50.8 \mu\text{m}$  ( $0.002 \text{ in.}$ ).

2) Electroless nickel-plated copper frame: Copper alloy C11000-H03 temper; the surface plating is electroless nickel, 5% phosphorous minimum,  $0.0015 \pm 0.0005 \text{ in.}$  with an oven bake at  $275 \pm 10^\circ\text{F}$  after 4 h. A yellow chromate conversion solution is applied. The surface roughness is  $0.6 \mu\text{m}$  ( $24 \mu\text{in.}$ ) with a surface flatness of  $0.254 \text{ mm}$  ( $0.010 \text{ in.}$ ).

3) Aluminum card rail: Aluminum alloy A356-T61 solution heat-treated and aged; the surface treatments were gold or silver films deposited on the aluminum surface and the optimum thicknesses of the coatings were determined as part of the present investigation in an effort to maximize the contact area. The surface roughness and flatness were maintained at  $0.6 \mu\text{m}$  ( $24 \mu\text{in.}$ ) and  $50.8 \mu\text{m}$  ( $0.002 \text{ in.}$ ), respectively, to be consistent with the specified surfaces.

Once the materials had been processed to required conditions, the various cylindrical test samples were then machined for further evaluation and testing.

#### Sample Preparation

All test specimens are  $2.54 \text{ cm}$  ( $1 \text{ in.}$ ) in diameter. The specimen that is inserted into the upper fixture is made from 6101-T6 aluminum. Its lower (test) end has been anodized to obtain a coating thickness of approximately  $85.1 \mu\text{m}$  ( $0.00335 \text{ in.}$ ). The specimen inserted into the lower fixture is made from C11000-H03 copper which has been nickel-plated to a thickness of approximately  $44.3 \mu\text{m}$  ( $0.00174 \text{ in.}$ ) on its upper (test) end. Both are  $10.16 \text{ cm}$  ( $4 \text{ in.}$ ) in length, this was calculated to be a length sufficient to ensure one-dimensional heat flux near their test ends. Inserted between the anodized 6101-T6 and nickel-plated copper specimens is a  $3.76\text{-cm}$

( $1.5\text{-in.}$ ) long sample of aluminum A356-T61. The ends of the A356 specimen are either bare or coated with approximately  $1\text{--}3 \mu\text{m}$  ( $40\text{--}120 \mu\text{in.}$ ) of vapor deposited gold or silver.

All specimens are instrumented with five chromel-alumel (type K) Teflon®-coated American wire gauge (AWG) 30 thermocouples. These thermocouples are special limit of error ( $\pm 1.1^\circ\text{C}$ , half of normal) grade. The thermocouples are inserted into holes in the specimens drilled to their axes with a no. 56 drill at  $0.635\text{-cm}$  ( $0.25\text{-in.}$ ) intervals along the specimen axes. Metallic powder (aluminum or copper to match the specimen base metal) is tamped into each hole to ensure that the thermocouple bead is thermally connected to all sides of the hole so that it provides a truly representative reading of the temperature in the material surrounding the hole. The thermocouples are connected to a Hewlett-Packard 3497A Data Acquisition control unit and an HP-87 terminal. The reference temperature is provided by a circuit in the HP-3497A.

#### Thermal Conductivity Calibration

The thermal conductivity of one sample from each of the three base materials (A356-T61, 6101-T6, C11000-H03) has been determined with the previously described apparatus, since accurate values of this property are needed to calculate the heat flux through the test junctions with sufficient accuracy.

Stainless steel (304) heat flux meters, used in place of the 6101-T6 and C11000 copper samples, were employed in determining the thermal conductivity of the three base materials. The stainless steel meters were calibrated by employing an electrolytic iron specimen of known conductivity as determined by the National Bureau of Standards/National Institute of Standards and Technology (NBS/NIST).<sup>15</sup> The experimentally determined thermal conductivities of the three base materials compare favorably to published values for similar alloys,<sup>16</sup> and are listed in Table 1.

#### Microhardness Measurements

##### Base Materials

The Vicker's microhardness of the three base materials was measured for three specimens from each material, all with a nominal surface roughness of  $0.6 \mu\text{m}$  ( $24 \mu\text{in.}$ ). These specimens were tested over a range of indenter loads from 10- to 500-gm force and the results are presented in Table 1.

Table 1 Thermal conductivity, Vicker's microhardness, and surface metrological data for test specimens

Base material-sample-surface <sup>a</sup>	Coating material	$k_s/k_c$ , <sup>b</sup> W/mK	$H_u/H_c$ , <sup>c</sup> kg/mm <sup>2</sup>	$t$ , $\mu\text{m}$	$R_a$ , $\mu\text{m}$	$R_q$ , $\mu\text{m}$	$W_a$ , $\mu\text{m}$	$W_q$ , $\mu\text{m}$	$F$ , $\mu\text{m}$	$S_q$ , rad
6101-F2	Anodized "hard coat"	208.4/0.0292	85/280	85.1	2.09	2.70	1.44	1.88	26.95	0.266
C110-F2	Electroless nickel plating	405.7/5.02	101/600	44.3	1.98	2.61	1.25	1.58	26.30	0.258
					0.12	0.16	0.77	0.86	4.45	0.031
A356-S3-AA	Bare	152.1/None	128/None	0	0.14	0.19	1.17	1.31	5.75	0.043
A356-S3-NC				0	1.04	1.20	0.55	0.67	9.10	0.139
A356-S11-AA	Vapor deposited gold	152.1/315	128/108	0	0.30	0.41	0.21	0.26	5.75	0.082
A356-S11-NC				1.00	0.54	0.70	0.93	1.12	8.90	0.103
A356-S10-AA				1.00	0.45	0.57	0.96	1.18	7.85	0.115
A356-S10-NC				2.01	0.46	0.59	0.68	0.86	8.05	0.100
A356-S12-AA				2.00	0.44	0.56	0.59	0.70	6.15	0.078
A356-S12-NC				3.01	0.52	0.67	1.28	1.59	10.70	0.114
A356-S5-AA	Vapor deposited silver	152.1/427	128/116	3.00	0.53	0.67	0.58	0.72	8.15	0.114
A356-S5-NC				1.00	0.69	0.81	0.40	0.49	7.30	0.115
A356-S4-AA				1.00	0.25	0.34	0.24	0.32	4.55	0.074
A356-S4-NC				2.00	0.15	0.22	0.58	0.70	5.10	0.071
A356-S6-AA				2.00	0.23	0.31	0.30	0.38	4.30	0.072
A356-S6-NC				3.00	0.35	0.44	0.39	0.52	4.55	0.088
				3.00	0.52	0.63	0.34	0.42	6.00	0.106

<sup>a</sup>AA and NC Denote surfaces in contact with anodized aluminum 6101 and electroless nickel-plated copper, respectively. The two rows of data for the anodized 6101 and copper specimens are for mutually perpendicular measurements across each of their surfaces.

<sup>b</sup> $k$  For anodic coating from Peterson and Fletcher,<sup>18</sup> and  $k$  for silver and gold from Touloukian and Ho.<sup>16</sup>

<sup>c</sup>Tabor<sup>17</sup> lists the hardness of annealed silver and cast gold as 25 and  $30 \text{ kg/mm}^2$ , respectively.

### Anodized/Plated/Coated Materials

The Vicker's microhardness was measured for the anodized aluminum, nickel-plated copper and silver- and gold-coated aluminum surfaces over a range of indenter loads from 10- to 500-gm force. The microhardness measurements as a function of indenter load are also presented in Table 1.

The Vickers hardness number (VHN) for the anodized aluminum 6101-T6 describes the range of measurements obtained for five coating thicknesses. The microhardness generally decreases with increasing coating thickness and increases slightly with increasing indenter load.

The microhardness for the electroless nickel-plated copper C11000-H03 for platings thicker than approximately 34  $\mu\text{m}$  (0.0013 in.) falls within the range of 540–630 VHN, well within the published range of 350–700 VHN for as-deposited platings.<sup>19,20</sup> The hardness of platings thinner than 34  $\mu\text{m}$  decreases with increasing indenter load, the load dependence being more pronounced for decreasing thicknesses. With thin platings the indenter deeply or completely penetrates the plating. When this occurs, the indicated hardness is influenced by the hardness of the soft copper substrate.

The Vicker's microhardness of vapor deposited silver- and gold-coated aluminum A356-T61 for three coating thicknesses is given in Table 1. The microhardness decreases with increasing coating thickness, as expected.

### Surface Measurements

The surface characteristics of the mating materials are particularly important in analyzing the heat transfer through a metallic junction. The actual contact pressure at the junction is highly dependent upon surface geometry, therefore, detailed surface information is essential for analysis. A surface profile for each surface was measured using a Surfanalyzer 5000/400 manufactured by Federal Products Corporation. A summary of the measurements is provided in Table 1.

A complete surface characterization was conducted, including measurements of the rms surface roughness, the average surface roughness (CLA), the average and rms waviness, the overall flatness deviation, and the rms asperity slope.

### Surface Coating

The experimental determination of the thermal contact resistance between the card guide chassis and the guide ribs of standard electronic modules involves anodizing or plating of the SEM card materials. The copper C11000-H03 was electroless nickel-plated using techniques described by Krieg<sup>21</sup> and a plating bath developed by Maclean and Karten,<sup>22</sup> and the aluminum alloy 6101-T6 was finished with a black anodic coating type III class 2 using a process described by Darrow.<sup>23</sup>

In order to provide for an optimization of the contact area between the card rails and the module guide ribs, samples of the A356-T61 aluminum card rail material were coated with vapor deposited silver and gold.

### Environmental Testing

Appropriate samples of the nickel-plated copper and anodized aluminum were subjected to a standard salt spray/fog test for 48 h, then evaluated for corrosion effects.<sup>24</sup> These surface coatings were found to exhibit no change as a result of the salt fog test. Although there are no environmental specifications for the vapor deposited silver- and gold-coated surfaces, these samples were subjected to the same salt fog test. These vapor deposited silver- and gold-coated A356 samples exhibited some flaking and peeling of the coating, possibly due to galvanic corrosion or hygroscopic adsorption.

### Experimental Procedure

An A356 specimen was placed between the 6101 and copper specimens, and an alignment fixture was then clamped around all three specimens. The adjustment nut on the top plate was turned to bring all specimens into contact and a preload of 862 kPa (125 psi) was applied. The alignment fixture was then

removed. Its use not only ensures precise mating of the specimens, but also eliminates any sliding of the specimens which might mar the soft gold and silver coatings on some of the A356 specimens. The radiation shield was installed around the test specimens, and was positioned so as to not come into contact with the specimens, since the shield would then behave as an unwanted heat sink.

After the thermocouple readings were checked, the test chamber was evacuated to a vacuum of  $1 \times 10^{-5}$  Torr or lower. Upon reaching the desired vacuum level the power to the heater was turned on and the heat sink temperature was set. Prior to taking data, the test samples were allowed to out-gas for approximately 6–8 h.

Temperature and pressure test conditions were set by adjusting the heater current and pressurizing the load bellows to an appropriate loading. Data were taken when the test sample temperatures did not vary more than  $\pm 0.3^\circ\text{C}$  over a period of 1 h.

### Data Analysis

Once the test column has reached a steady-state temperature profile, which is taken as a  $\pm 0.3^\circ\text{C}$  or smaller change in any given thermocouple reading over a period of 1 h, a data retrieval and analysis program is executed. The data acquisition program includes the temperature data, load data, and other information, and computes the heat flux through both test samples. The heat flux is computed using the temperature gradient obtained by linear least squares fit of the temperatures, and the thermal conductivities of the specimens at their respective mean temperatures, as calculated using the thermal conductivity correlation and interpolation program developed from the calibration of the test sample materials. The heat flux across each junction is computed as the average of the heat flux through the specimens on either side of the interface. The temperature discontinuity across the interface is obtained by extrapolating the temperatures within the specimens to the interface. The contact conductance is computed to be the average heat flux across the interface divided by the change in temperature across the junction.

### Uncertainty

An experimental investigation is not complete without estimation of the uncertainties associated with the measured quantities and the resulting calculated values. The uncertainty in a particular result may be determined in terms of the measured quantities. The technique used to calculate the uncertainty values follows that of Kline and McClintock.<sup>25</sup>

The uncertainty in the thermal conductivity of the base materials used in the investigation was determined to be 2.46% for the aluminum alloy A356-T61, 2.76% for the aluminum 6101-T6, and 4.18% for the copper C11000-H03. The resulting thermal conductivity values were used in the experimental measurements of the thermal contact conductance of the coated surfaces.

The uncertainty in the thermal contact conductance is of particular importance, and relative uncertainty estimates have been calculated. The uncertainty in the contact conductance of the anodized aluminum 6101 to the bare aluminum A356 is calculated to be 4.93%, and for the electroless nickel-plated copper C11000 to the bare A356 is determined as 10.53%. For the silver- and gold-coated aluminum A356 junctions, the uncertainty in the conductance for the anodized aluminum 6101 to the silver- or gold-coated aluminum A356 is calculated to be 4.20%, and for the nickel-plated copper C11000 to the coated aluminum A356 it is determined to be 6.73%.

### Results and Discussion

In order to improve the overall thermal performance of existing card/rail interfaces, it is important to document the thermal characteristics of the card/rail materials. Based on these baseline thermal performance characteristics, it is then possible to experimentally determine potential improvements in the overall thermal performance with coated surfaces. This

investigation involves the experimental determination of the baseline thermal contact conductance for anodized aluminum 6101-T6 and electroless nickel-plated copper C11000-H03 card materials to aluminum alloy A356-T61 rail material, then experimental conductance measurements of the card/rail interfaces with the rail surface coated with vapor-deposited silver or gold.

#### Baseline Contact Conductance Results

The anodized aluminum 6101-T6 and nickel-plated copper alloy C11000-H03 thermal contact conductance data are presented in Figs. 3 and 4 as a function of contact pressure and mean interface temperature. Contact pressures were varied from 0.172–0.862 MPa (25–125 psi), and temperatures were varied from 20 to 100°C (68–212°F).

The thermal contact conductance data for the anodized aluminum 6101-T6 to bare aluminum A356-T61 varies from 25 to 92 W/m<sup>2</sup>K (4.4–16 Btu/hft<sup>2</sup>°F) over the range of parameters tested (Fig. 3). The magnitude of these conductance values is reasonable, considering that the anodized aluminum surface acts as an insulator, limiting the heat transfer. Furthermore, the anodized coating is a hard anodization, which limits the actual contact area.

The thermal contact conductance data for the electroless nickel-plated copper alloy C11000-H03 are substantially larger than the anodized coating data, ranging from 600 to 2800 W/m<sup>2</sup>K (106 to 493 Btu/hft<sup>2</sup>°F) (Fig. 4). The metal-to-metal interface improves the overall conductance, even though the nickel plating is hard.

Note that the contact conductance curve for the 20°C series of tests for the nickel-plated C11000 to bare A356-T61 junction is higher than the curve for the 40°C series. This may be due to the temperature gradient in the copper heat fluxmeter

being too small to provide an accurate estimation of the heat flux at 20°C. More specifically, the ethylene glycol circulated through the cooling coils was maintained at approximately –10°C. The heat removal capacity will only accommodate a small heat flux at the heated end of the test column if the mean interface temperature is to be maintained at 20°C. Small heat fluxes produce small temperature gradients through the test column. As a consequence, signal noise could effect the temperature readings, greatly influencing the computed values of the small temperature gradient. For the case of the 20°C curve it is believed that the computed gradient is too large, causing the contact conductance to be overestimated.

Note that for both junction types the contact conductance increases substantially with increasing pressure. The conductance also increases significantly with temperature, although the effect of temperature is less pronounced than that of apparent contact pressure. The increase of conductance with pressure is due to increased deformation of the surface asperities. The increase in conductance with temperature is possibly due in large-part to a reduction in the hardness of the materials, particularly the aluminum A356-T61, rather than thermal distortions of the contacting surfaces.

While there have been very few experimental investigations of anodized aluminum to bare aluminum interfaces, there has been one investigation utilizing comparable anodization thicknesses and test conditions. Peterson and Fletcher<sup>18</sup> investigated the thermal contact conductance and thermal conductivity of several different thickness anodized coatings. The experimental thermal conductance values of the present investigation are compared with those of Peterson and Fletcher<sup>18</sup> in Fig. 3, for comparable anodization thicknesses. While the data magnitude and trends are similar, the mean junction temperature of the Peterson and Fletcher data was lower; however, their anodization process was also different than that used for specimens in the present investigation.

#### Contact Conductance for Silver Coatings

The thermal contact conductance data for the anodized aluminum 6101 and electroless nickel-plated copper to aluminum A356-T61 junctions are presented in Figs. 5 and 6 as a function of coating thickness, contact pressure, and mean interface temperature. Initial tests were conducted with three different thickness coatings, in order to determine the optimum coating thickness for each junction. Subsequently, a series of tests employing the coatings of optimum thickness were conducted for additional interface temperatures for both anodized aluminum and nickel-plated copper in contact with the vapor-deposited silver-coated aluminum.

The contact conductance of both junctions is observed to increase significantly with pressure. This is due to the increased number and area of contacts brought about by the deformation of the surfaces, and especially the coatings, under higher pressures. Note that for the anodized aluminum 6101

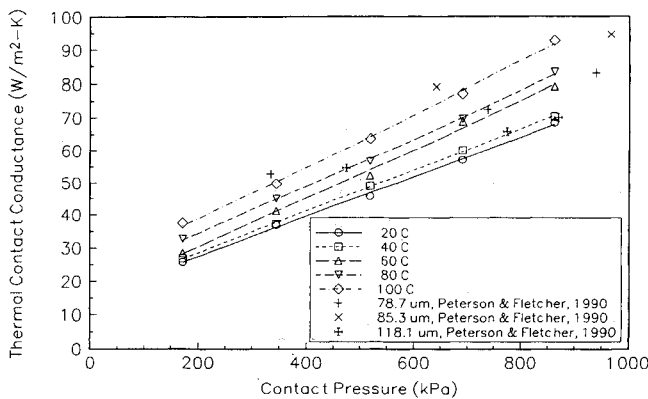


Fig. 3 Thermal contact conductance as a function of pressure and temperature for anodized aluminum 6101-T6 to uncoated aluminum alloy A356-T61 including a comparison of the present experimental data with published data.

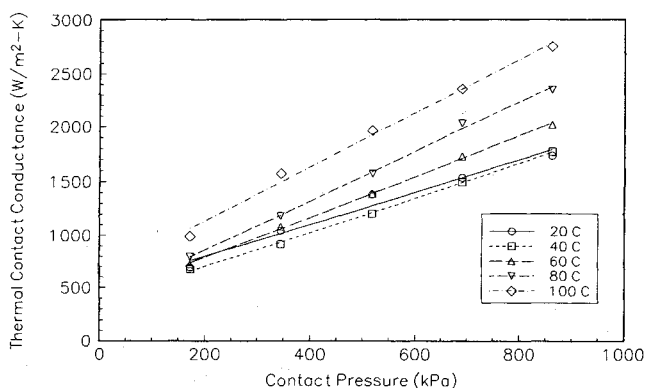


Fig. 4 Thermal contact conductance as a function of pressure and temperature for electroless nickel-plated copper alloy C11000-H03 to uncoated aluminum alloy A356-T61.

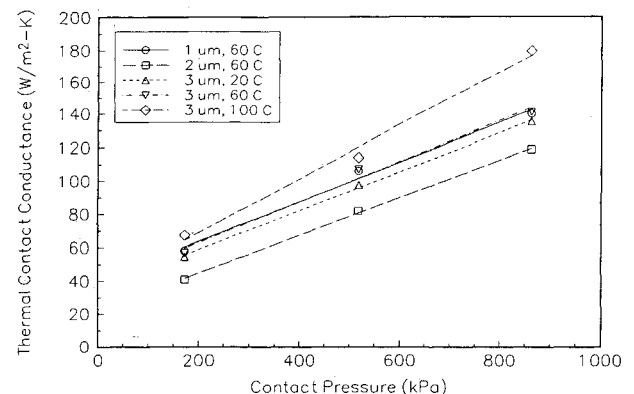


Fig. 5 Thermal contact conductance of anodized aluminum 6101-T6 to silver-coated aluminum alloy A356-T61 as a function of pressure for selected silver coating thicknesses.

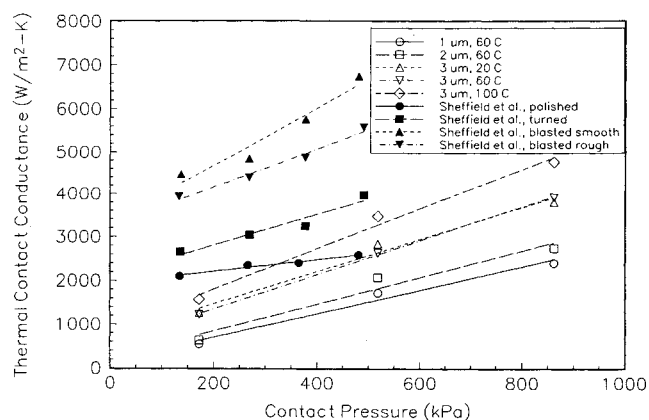


Fig. 6 Thermal contact conductance of electroless nickel-plated copper alloy C11000-H03 to silver-coated aluminum alloy A356-T61 as a function of pressure for selected silver coating thicknesses, including a comparison with published experimental data.

to silver-coated aluminum A356 junction, the lines for the 1-, 2-, and 3- $\mu$ m coatings have nearly identical slopes (Fig. 5). Also, the 1- and 3- $\mu$ m lines are almost coincident, while the 2- $\mu$ m line is lower. For the nickel-plated copper C11000 to coated aluminum A356 junction, the conductance increases monotonically with coating thickness (Fig. 6).

For identical surface profiles the conductance typically increases with coating thickness (for coatings softer than the substrate) until the bulk resistance of the coating counters the increase in conductance afforded by the coating, as noted by Kang et al.<sup>10</sup> They noted that the optimum thickness ranged from 0.5 to 2  $\mu$ m for indium, tin, and lead coatings. However, the gold and silver coatings employed in the present investigation are many times more conductive than the coatings used by Kang et al.<sup>10</sup> Hence, the bulk resistance of the vapor-deposited gold and silver coatings should not become dominant until they are applied in much greater thicknesses. The expected trend would be that of increasing conductance with thickness well beyond 3  $\mu$ m.

Deviations of the observed behavior from that expected are probably in large-part due to differences in surface profile of the specimens (refer to Table 1). In the case of the anodized aluminum 6101 to the silver-coated aluminum A356 junction, the surface of the 1- $\mu$ m silver-coated specimen was quite flat, allowing mating of the surfaces across their entire diameters. The surface of the 2- $\mu$ m silver-coated aluminum A356 specimen exhibited significant crowning (i.e., an elevation of the center of a surface above that surrounding it). This would prohibit contact over the annulus surrounding the raised (crowned) portion of the surface, causing decreased conductance. The 3- $\mu$ m silver-coated aluminum A356 surface was somewhat less crowned than the 2- $\mu$ m coated surface, resulting in a less constricted contact than for the 2- $\mu$ m coated surface. With regard to the electroless nickel-plated copper C11000 to silver-coated aluminum A356 junction, the 1- $\mu$ m silver-coated aluminum A356 surface was essentially flat, while those of the 2- and 3- $\mu$ m coated surfaces showed slight crowning.

It is not altogether clear how the differences in roughness of the silver-coated aluminum A356 surfaces may affect the conductance. Chung et al.<sup>11</sup> argue that increases in roughness, while remaining less than the coating thickness, cause increases in conductance due to the increased contact along the sides of the microscopic asperities. Waviness may affect how groups of asperities make contact, the contact area decreasing with increasing waviness. For the anodized aluminum 6101 to aluminum A356 junction, the waviness of the 1- $\mu$ m coated surface was considerably less than half that of the 2- $\mu$ m coated surface, while the waviness of the 3- $\mu$ m coated surface was approximately equal to that of the 1- $\mu$ m coated surface. The trend in waviness observed for the silver-coated aluminum

A356 surfaces in contact with the electroless nickel-plated copper C11000 was that of slightly increasing waviness with increasing coating thickness.

Since the 3- $\mu$ m-thick silver coating showed the greatest contact conductance for both junctions, as expected, it was chosen for more complete characterization at additional temperatures (i.e., 20 and 100°C). The increase in contact conductance with increasing pressure is slightly more pronounced for higher interface temperatures (Figs. 5 and 6). The conductance of both junction types increases significantly as the junction temperature is increased from 60 to 100°C, although it varies only slightly from 20 to 60°C.

Also shown in Fig. 6 are contact conductance data obtained by Sheffield et al.<sup>7</sup> for vapor-deposited silver coatings on one surface of aluminum 6061-T651 contact pairs exhibiting four widely varying roughnesses, as shown in Fig. 6. These data were obtained at a mean interface temperature of 60°C. Note that the conductance values reported by Sheffield et al.<sup>7</sup> generally increase with increasing roughness and are significantly greater than the data obtained in the present investigation. The aluminum 6061-T651 specimens that Sheffield et al.<sup>7</sup> tested were softer than the aluminum A356-T61 and considerably softer than the electroless nickel-plated copper employed in this investigation. This assertion is supported by their bare junction results (not shown) which are considerably greater than the bare junction data for this investigation.

#### Contact Conductance for Gold Coatings

The thermal contact conductance data for the anodized aluminum 6101 and the electroless nickel-plated copper C11000 in junction with the vapor deposited gold-coated aluminum A356 are plotted in Figs. 7 and 8. In a method analogous to the experiments involving vapor deposited silver coatings, three different thicknesses of vapor deposited gold were tested for the purpose of determining the optimum thickness for each junction, then a series of tests utilizing these optimum thicknesses were performed for the anodized aluminum 6101 and electroless nickel-plated copper C11000 to vapor deposited gold-coated aluminum A356 contacts.

In the case of the anodized aluminum 6101 to vapor deposited gold-coated aluminum A356 junction, the contact conductance increases slightly for an increase in coating thickness from 1 to 2  $\mu$ m (Fig. 7). The conductance is significantly increased by further increasing the coating thickness to 3  $\mu$ m. The surface roughnesses were similar for all three vapor deposited gold-coated aluminum A356 surfaces in contact with the anodized aluminum 6101. All three surfaces were crowned; however, the 2- $\mu$ m gold-coated surface exhibited a small rounded peak which may have prevented contact across the entire surface. This may explain why the conductance of the junction with the 2- $\mu$ m vapor deposited gold coating was only slightly greater than the conductance of the 1- $\mu$ m gold-coated junction, yet markedly less than the conductance of the 3- $\mu$ m

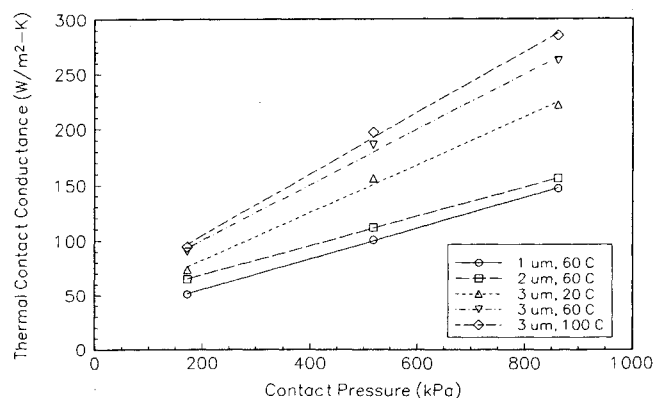


Fig. 7 Thermal contact conductance of anodized aluminum 6101-T6 to gold-coated aluminum alloy A356-T61 as a function of pressure for selected gold coating thicknesses.

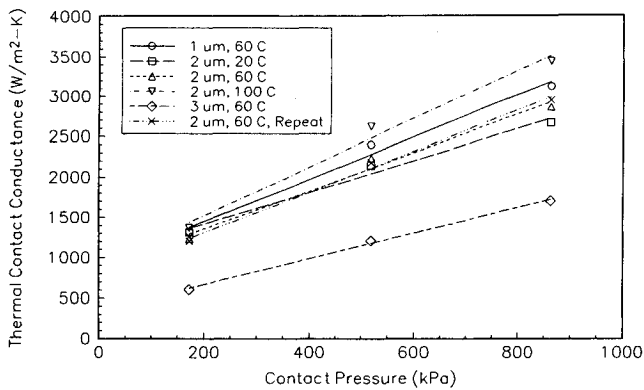


Fig. 8 Thermal contact conductance of electroless nickel-plated copper alloy C1100-H03 to gold-coated aluminum alloy A356-T61 as a function of pressure for selected gold coating thicknesses.

gold-coated contact. The anodized aluminum 6101 to 3-μm vapor deposited gold-coated aluminum A356 junction was selected for further testing at 20 and 100°C because it provided the greatest conductance. Also, as shown in Fig. 8, the conductance at the junctions between the electroless nickel-plated C11000 and 1- and 2-μm-thick vapor deposited gold-coated A356 are nearly equal, while the conductance of the junction employing the 3-μm vapor deposited gold-coated A356 is considerably smaller. All three vapor deposited gold-coated aluminum A356 surfaces tested in contact with the nickel-plated copper C11000 exhibited similar surface roughness, waviness, and flatness measurements. Hence, an explanation of this observed behavior based on the effects of surface measurements is unavailable. The 2-μm gold coating was chosen for further testing at 20 and 100°C, since the usually observed trend is for conductance to increase with thickness of the vapor deposited soft metal coating.

The conductance of the anodized aluminum 6101 junction increases slightly more rapidly with pressure for higher interface temperatures, while no definite similar trend is observed for the nickel-plated copper junction (Figs. 7 and 8). Also, for a given contact pressure, the conductance of both junctions generally remains approximately constant or increases with temperature. An additional series of tests was performed at 60°C for the nickel-plated copper to gold-coated aluminum A356 junctions (Fig. 8). This additional series was performed in order to evaluate the repeatability of the data. This involved removal and reinsertion of the 2-μm vapor deposited gold-coated aluminum A356 specimen to establish an entirely new contact configuration. The maximum difference between corresponding data pairs (i.e., equal pressure) was 3.0%. This is less than the calculated uncertainty in the contact conductance of junctions employing vapor deposited silver and gold coatings (6.73%).

#### Thermal Enhancement of Silver and Gold Coatings

This investigation has experimentally determined that vapor deposited coatings of both silver and gold do indeed, as predicted, significantly increase the contact conductance of the SEM frame/card rail interface.

#### Vapor Deposited Silver Coatings

The contact conductance ratios for vapor deposited silver-coated to uncoated aluminum A356 are illustrated in Fig. 9. For the anodized aluminum 6101 to aluminum A356 junction the conductance ratio, or enhancement factor, ranges from 1.79 to 2.14 for the 3-μm-thick silver coating. The conductance ratio decreases slightly with increasing pressure for mean interface temperatures of 20 and 60°C, and increases slightly with pressure at 100°C. No definite dependence of the conductance ratio on temperature is evident. The 20 and 100°C curves cross at higher apparent contact pressures, but are within the range of uncertainties for the experimental con-

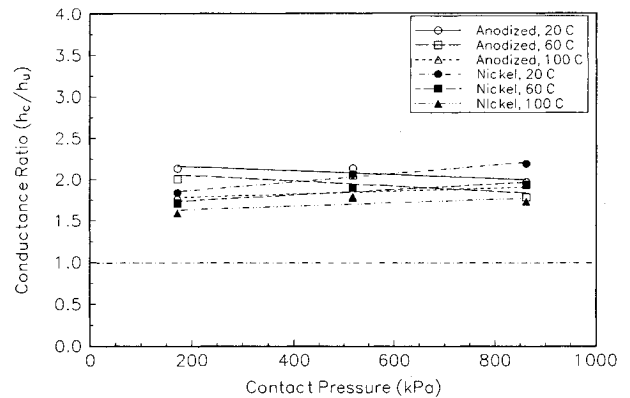


Fig. 9 Comparison of the ratio of coated to uncoated thermal contact conductance for anodized aluminum 6101-T6 to 3-μm silver-coated aluminum A356-T61 and nickel-plated copper C11000-H03 to 3-μm silver-coated aluminum A356-T61.

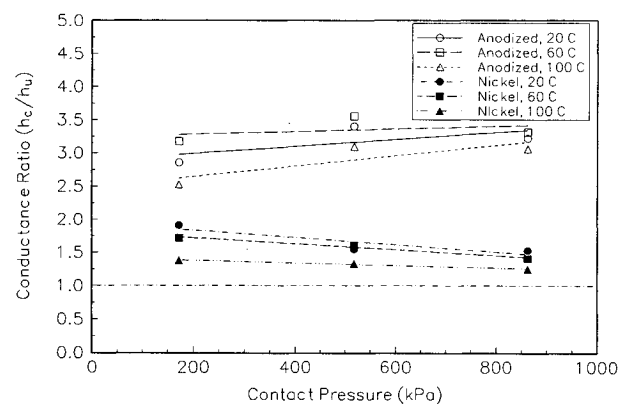


Fig. 10 Comparison of the ratio of coated to uncoated thermal contact conductance for anodized aluminum 6101-T6 to 3-μm silver-coated aluminum A356-T61 and nickel-plated copper C11000-H03 to 2-μm gold-coated aluminum A356-T61.

ductance data. As for the electroless nickel-plated C11000 copper to aluminum A356 junction, the coated/uncoated conductance ratio ranges from 1.59 to 2.19 for the 3-μm silver coating. The conductance ratio increases moderately with pressure for all three temperatures, but again, no dependence on temperature is evident.

#### Vapor Deposited Gold Coatings

Figure 10 portrays the conductance ratios for vapor deposited gold-coated to uncoated aluminum A356. The conductance ratio for the anodized aluminum 6101 to aluminum A356 ranges from 2.53 to 3.41 for the 3-μm gold coating. The ratio decreases with increasing temperature for a given pressure. Also, a maximum ratio is observed at a pressure of 75 psi for each of the three mean interface temperatures. For the electroless nickel-plated copper C11000 to aluminum A356 junction, the conductance ratio ranges from 1.25 to 1.91 for the 2-μm vapor deposited gold coating. The ratio decreases significantly with increasing temperature for a given pressure. It also decreases moderately with increasing pressure for a given temperature.

#### Conclusions and Recommendations

The standard electronic module overall temperature may be reduced through thermal enhancement of the interface between the card guide chassis and the guide ribs of the modules. Thermal enhancement may be accomplished through metallic coatings applied to the card rails.

In order to substantiate the suitability of silver and gold for thermal enhancement of SEM card/rail interfaces, an experimental investigation was conducted. Experimental thermal conductance measurements were made for anodized alumi-

num 6101-T6 and electroless nickel-plated copper C11000-H03 frame materials to the aluminum A356-T61 rail material. Experimental thermal conductance values of vapor deposited silver- and gold-coated aluminum A356-T61 rail surfaces were greater than conductance values for the uncoated A356 by factors of 1.79–2.14 (3- $\mu\text{m}$  silver coating), and 2.53–3.41 (3- $\mu\text{m}$  gold coating) for the anodized aluminum 6101 to A356 junction. The enhancement factors for the electroless nickel-plated copper to A356 junction were 1.59–2.19 (3- $\mu\text{m}$  silver coating), and 1.25–1.91 (2- $\mu\text{m}$  gold coating).

Although the vapor deposited silver and gold coatings for the aluminum A356 afforded significant enhancement of the thermal contact conductance, these coating/basis metal combinations are susceptible to galvanic corrosion as determined by the salt spray/fog test. The vapor deposited silver and gold coatings were 1–3  $\mu\text{m}$  in thickness, and so were not thick enough to entirely cover small flaws on the A356 substrate. Perhaps more heavily applied coatings of vapor deposited silver or electroplated silver coatings may provide the necessary corrosion resistance. Electroplated silver coatings are typically harder than vapor deposited silver coatings, yet may still yield markedly increased conductance. Such heavily applied coatings of gold may prove to be prohibitively expensive.

The use of thicker, softer anodic coatings, such as those applied at room temperature, for the 6101-T6 aluminum, instead of the currently used type III, class 2 (hard coat, chilled processing) coating, may increase the contact conductance of the anodized aluminum 6101 to aluminum A356 junction.

Replacement of the anodized coating on the aluminum 6101 with a chromate conversion coating may also significantly increase the contact conductance of the frame/card rail junction. Chromate conversion coatings are typically only a few Ångströms thick, and possess a much smaller bulk resistance than thick anodic coatings. Conversion coatings are also softer than anodic coatings. There is a possibility that a chromate conversion coating on the 6101 aluminum frame material may be penetrated by microscopic surface asperities on the surfaces of the aluminum A356 card rail and aluminum wedge clamp. However, since all three components comprising the junction (the frame, card rail, and wedge clamp) are fabricated from aluminum alloys, galvanic corrosion may not present a problem.

### Acknowledgments

Support for this study was provided by the Office of Naval Technology, Washington, DC, through NSWC Contract N00164-91-C-0043 and the Texas A&M University Center for Space Power.

### References

- <sup>1</sup>Kraus, A. D., and Bar-Cohen, A., *Thermal Analysis and Control of Electronic Equipment*, Hemisphere, New York, 1983.
- <sup>2</sup>Fried, E., "Study of Interface Thermal Contact Conductance," G. E. Valley Forge Space Technology Center, Summary Rept., G. E. Document 65S04395, Philadelphia, PA, 1965.
- <sup>3</sup>Fried, E., and Kelly, M. J., "Thermal Conductance of Metallic Contacts in a Vacuum," AIAA Paper 65-661, Sept. 1965.
- <sup>4</sup>Mal'kov, V. A., and Dobashin, P. A., "The Effect of Soft-Metal Coatings and Linings on Contact Thermal Resistance," *Inzhenerno-Fizicheskii Zhurnal*, Vol. 17, No. 5, 1969, pp. 871–879.
- <sup>5</sup>Mikic, B. B., and Carnasciali, G., "The Effect of Thermal Conductivity of Plating Material on Thermal Contact Resistance," ASME Winter Annual Meeting, American Society of Mechanical Engineers Paper 69-WA/HT-9, Los Angeles, CA, Nov. 1969.
- <sup>6</sup>O'Callaghan, P. W., Snaith, B., Probert, S. D., and Al-Astrabadi, F. R., "Prediction of Optimal Interfacial Filler Thickness for Minimum Thermal Contact Resistance," AIAA Paper 81-1166, June 1981.
- <sup>7</sup>Sheffield, J. W., Williams, A., Sauer, H. J., Jr., O'Keefe, T. J., and Chung, K. C., "Enhancement of Thermal Contact Conductance by Transitional Buffering Interfaces (TBI)," NSF Final Project Rept., NSF Grant CTS-8901871, Univ. of Missouri at Rolla, MO, Jan. 1992.
- <sup>8</sup>Antonetti, V. W., and Yovanovich, M. M., "Enhancement of Thermal Contact Conductance by Metallic Coatings: Theory and Experiment," *Journal of Heat Transfer*, Vol. 107, Aug. 1985, pp. 513–519.
- <sup>9</sup>Antonetti, V. W., and Yovanovich, M. M., "Using Metallic Coatings to Enhance Thermal Contact Conductance of Electronic Packages," *Heat Transfer Engineering*, Vol. 9, No. 3, 1988, pp. 85–92.
- <sup>10</sup>Kang, T. K., Peterson, G. P., and Fletcher, L. S., "Enhancing the Thermal Contact Conductance Through the Use of Thin Metallic Coatings," *Transactions of the American Society of Mechanical Engineers, Journal of Heat Transfer*, Vol. 112, No. 4, 1990, pp. 864–871.
- <sup>11</sup>Chung, K. C., Sheffield, J. W., and Sauer, H. J., Jr., "Effects of Metallic Coated Surfaces on Thermal Contact Conductance: An Experimental Study," 6th Miami International Symposium on Heat and Mass Transfer, Miami Beach, FL, Dec. 1990.
- <sup>12</sup>Chung, K. C., Sheffield, J. W., Sauer, H. J., Jr., and O'Keefe, T. J., "The Effects of Transitional Buffering Interface Coatings on Thermal Contact Conductance," AIAA Paper 91-0490, June 1991.
- <sup>13</sup>Lambert, M. A., and Fletcher, L. S., "A Review of the Thermal Contact Conductance of Junctions with Metallic Coatings and Films," AIAA Paper 92-0709, Jan. 1992.
- <sup>14</sup>Lambert, M. A., and Fletcher, L. S., "Thermal Enhancement Techniques for SEM Guide Rails and Card Rails: 1991 Annual Report," Conduction Heat Transfer Lab., Dept. of Mechanical Engineering, Texas A&M Univ., Rept. CHTL-6770-6, College Station, TX, 1992.
- <sup>15</sup>Lust, J. G., and Lankford, A. B., "Update of Thermal Conductivity and Electrical Resistivity of Electrolytic Iron, Tungsten and Stainless Steel," U.S. Dept. of Commerce/National Bureau of Standards Special Publication 260-90, Washington, DC, Sept. 1984.
- <sup>16</sup>Touloukian, Y. S., and Ho, C. Y. (eds.), *Thermophysical Properties of Matter: Thermal Conductivity of Metallic Solids*, Vol. 1, Plenum Press, New York, 1972.
- <sup>17</sup>Tabor, D., *The Hardness of Metals*, Oxford Univ. Press, Amen House, London, 1951.
- <sup>18</sup>Peterson, G. P., and Fletcher, L. S., "Measurement of the Thermal Contact Conductance and Thermal Conductivity of Anodized Aluminum Coatings," *Transactions of the American Society of Mechanical Engineers, Journal of Heat Transfer*, Vol. 112, No. 3, 1990, pp. 579–585.
- <sup>19</sup>Brenner, A., "Electroless Plating Comes of Age," *Metal Finishing*, Vol. 52, No. 11, 1954, p. 68.
- <sup>20</sup>Brenner, A., Couch, D. F., and Williams, E. K., "Electrodeposition of Alloys of Phosphorus and Nickel or Cobalt," *Journal of Research*, National Bureau of Standards (RP 2061), Vol. 44, Jan. 1950, p. 109.
- <sup>21</sup>Krieg, A., "Processing Procedures," *Proceedings of the Symposium on Electroless Nickel Plating*, American Society for Testing and Materials STP 265, Philadelphia, PA, 1959, pp. 21–37.
- <sup>22</sup>Macleay, J. D., and Karten, S. M., "A Practical Application of Electroless Nickel Plating," *Plating*, Vol. 41, No. 11, 1954, p. 1284.
- <sup>23</sup>Darrow, G. R., "Engineering the Sulfuric Anodic Process," *Anodized Aluminum*, American Society for Testing and Materials STP 388, Philadelphia, PA, 1965, pp. 62–84.
- <sup>24</sup>"Standard Method of Salt Spray (Fog) Testing," American Society for Testing and Materials B117, Philadelphia, PA, Vol. 7, 1973, pp. 60–67.
- <sup>25</sup>Kline, S. J., and McClintock, F. A., "Describing Uncertainties in Single-Sample Experiments," *Mechanical Engineering*, Vol. 75, No. 1, 1953, pp. 3–8.